

## Self-Assembled Polymeric Supramolecular Frameworks\*\*

Nikolay Houbenov,\* Johannes S. Haataja, Hermis Iatrou, Nikos Hadjichristidis, Janne Ruokolainen, Charl F. J. Faul,\* and Olli Ikkala\*

Supramolecular framework materials with well-defined solvent-free or solvent-swollen cage-like cavities<sup>[1]</sup> are relevant in many fields of science and technology, for example, in chemical synthesis,<sup>[2]</sup> stabilization and hosting of delicate materials,<sup>[3]</sup> absorption of gases,<sup>[4]</sup> and functional materials.<sup>[5]</sup> More generally, controlled porosity is significant for, for example, supercapacitors<sup>[6]</sup> and low-dielectric-constant materials for electronics.<sup>[7]</sup> Within supramolecular chemistry, crystal engineering opens generic routes for the crystalline assembly of low-molecular-weight construction units in architecturally controlled frameworks<sup>[1,2,8]</sup> through reversible intermolecular interactions, such as coordination bonds,<sup>[5]</sup> metallo-organic constructs,<sup>[9]</sup> dipole–dipole coupling,<sup>[8b]</sup> hydrogen bonds,<sup>[8]</sup> and their combinations.<sup>[8,10]</sup> However, growth of supramolecular framework single crystals from oligomers is a slow and delicate process, which encourages the search for robust approaches based on polymers. Different concepts have been described: porous structures obtained by 1) 2D polyaddition and polycondensation for condensed carbon nitrides,<sup>[11a]</sup> 2) trimerization of aromatic nitriles for covalent triazine frameworks,<sup>[11b,c]</sup> or 3) co-condensation of boronic acids with hexahydroxy triphenylene for covalent organic frameworks<sup>[11d]</sup> all exhibit excellent properties for heterogeneous catalysis and H<sub>2</sub>, CH<sub>4</sub>, and CO<sub>2</sub> uptake, but the synthetic routes may be complex and costly in energy.

Rigid macromolecular backbones generate microvoids<sup>[12]</sup> caused by packing frustrations but lack well-defined pores. Finally, controlled 2D lattices of cylindrical pores can be

obtained by block copolymers with self-assembled domains that can be emptied.<sup>[13]</sup>

Encouraged by the progress in supramolecular concepts in polymer science,<sup>[14]</sup> one could expect that such concepts may lead to robust and well-defined cage-like solids upon self-assembly. Such materials have, however, not yet been reported for organic polymers.<sup>[15]</sup> Herein, our hypothesis was that the combination of the rigidity of  $\beta$ -sheet and  $\alpha$ -helical polypeptide structural motifs with orthogonal DNA-like hydrogen-bonding tectons and hierarchical self-assembly would lead to packing frustrations caused by competing shape-persistent motifs, and could thus generate well-defined polymeric framework solids. Such a structure could be denoted as a “molecular woodpile”. The feasibility of such an approach is suggested by our previous investigations into the triblock copolypeptide poly(L-lysine)-*block*-poly( $\gamma$ -benzyl-L-glutamate)-*block*-poly(L-lysine) (PLL-*b*-PBLG-*b*-PLL), which forms fibrillar networks through structuring over several length scales upon ionically complexing 2'-deoxyguanosine 5'-monophosphate (dGMP) to the PLL blocks.<sup>[16]</sup>

Herein, a diblock copolypeptide poly( $\gamma$ -benzyl-L-glutamate)-*block*-poly(L-lysine) (PBLG-*b*-PLL) is used (see the Supporting Information). dGMP is ionically complexed to the PLL (see Figure 2a); the complexation between the PLL amine and phosphoric acid is suggested by FTIR and elemental analysis (see the Supporting Information). FTIR is also used to resolve the polypeptide secondary structures.<sup>[17]</sup> The major absorption bands (amide I and amide II), show the presence of both  $\alpha$  helices and  $\beta$  sheets in the complexes. The  $\alpha$ -helical bands are assigned to PBLG, which is a prototypical  $\alpha$ -helical polypeptide.<sup>[18]</sup> The  $\beta$ -sheet structures are assigned to PLL (more details in Figure S1 in the Supporting Information). For simplicity, we will denote the complex as PBLG-*b*-PLL(dGMP).

Small-angle X-ray scattering (SAXS) shows reflections for PBLG-*b*-PLL(dGMP) at  $q_1 = 0.02 \text{ \AA}^{-1}$ , as well as higher-order reflections at  $3q_1$ ,  $5q_1$ , and  $7q_1$  (Figure 1a). This result indicates lamellar self-assembly at the polymeric scale with a periodicity of 31 nm,<sup>[19]</sup> as confirmed by cryo-TEM (Figure 1b).

From the molecular characteristics of the PBLG block (molecular weight and length of the helical pitch,  $l = 1.5 \text{ \AA}$ <sup>[20]</sup>) we estimate the thickness of the PBLG domain to be approximately 11 nm.<sup>[19]</sup> At the largest scale (31 nm) the PBLG-*b*-PLL(dGMP) therefore undergoes lamellar self-assembly with the PBLG domains approximately 11 nm thick, and the total thickness of a PLL(dGMP) layer is approximately 20 nm. The PBLG-*b*-PLL(dGMP) units are expected to pack in an antiparallel orientation, because no

[\*] Dr. N. Houbenov, J. S. Haataja, Prof. J. Ruokolainen, Prof. O. Ikkala  
Department of Applied Physics  
Aalto University School of Science and Technology  
(previously Helsinki University of Technology)  
P.O.Box 15100, 00076 Espoo (Finland)  
Fax: (+358) 9-4702-3155  
E-mail: houbenov@gyroid.hut.fi  
olli.ikkala@tkk.fi

Dr. H. Iatrou, Prof. N. Hadjichristidis  
Department of Chemistry, University of Athens (Greece)  
Dr. C. F. J. Faul  
School of Chemistry, University of Bristol (UK)  
and  
Bristol Centre for Nanoscience and Quantum Information  
University of Bristol (UK)  
E-mail: charl.faul@bristol.ac.uk

[\*\*] We are grateful to P. Hiekkataipale for assistance with SAXS. We acknowledge funding from the Academy of Finland (O.I., N.H., J.R.) and Nokia Research Center. C.F.J.F. acknowledges the University of Bristol for financial support and Aalto University for a visiting professorship.

Supporting information for this article is available on the WWW under <http://dx.doi.org/10.1002/anie.201007185>.

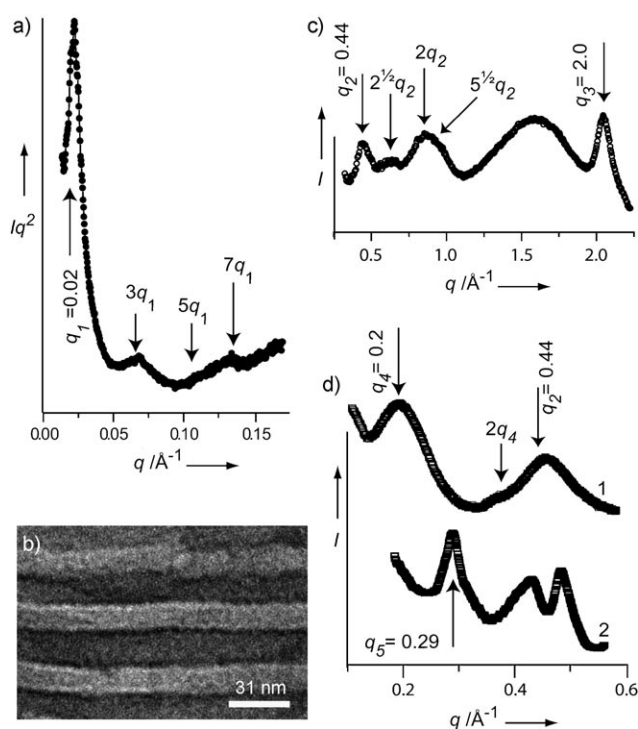


**Figure 1.** X-ray and TEM results for PBLG-*b*-PLL(dGMP). a) SAXS patterns confirming the 31 nm period of lamellar self-assembly. b) Cryo-TEM showing lamellar self-assembly of the RuO<sub>4</sub> stained blocks with similar main period. Light lamellae are assumed to present the PBLG domains, dark lamellae show the PLL(dGMP) domains. c) WAXS showing the tetragonal packing of PBLG helices and  $\pi$  stacking between G-ribbon plates. d) SAXS revealing a lamellar phase, caused by the formation of G-ribbon between the PLL  $\beta$ -sheets (curve 1). For comparison, curve 2 shows the uncomplexed dGMPs.

broken symmetry is to be expected for the PBLG dipole moments (see Figure 2b). This arrangement has an important implication for the packing: hexagonal packing of the PBLG helices could be a priori expected, but alternating dipole moments in a helical arrangement are not allowed in this symmetry. X-ray analysis provides clues as to how these constraints are alleviated: Figure 1c shows reflections at  $q_2 = 0.44 \text{ \AA}^{-1}$  (see also Figure 1d), as well as higher-order reflections at  $2^{1/2}q_2$ ,  $2q_2$ , and a weak reflection at  $5^{1/2}q_2$ . This observation indicates tetragonal packing of PBLG cylinders in alternate directions (see Figure 2b,c); the diameter of a single cylinder is approximately 1.5 nm, deduced from  $q_2$ .

The calculated length of a fully extended PLL  $\beta$  strand is approximately 31 nm and FTIR suggests that PLL adopts an antiparallel  $\beta$ -sheet secondary structure (see the Supporting Information). Based on geometry arguments and SAXS data, the thickness of a single layer of PLL(dGMP) is suggested to be 10 nm (i.e., half of the total PLL(dGMP) layer thickness). Therefore, two turns of each individual elongated PLL chain are expected, which leads to three antiparallel PLL chains within the  $\beta$  sheet (see Figure 2b). Taking the typical hydrogen bond lengths into account,  $\beta$  sheets with a length of 10 nm and a width of 1.38 nm are expected. Finally, Figure 1d (curve 1) shows a SAXS reflection at  $q_4 = 0.2 \text{ \AA}^{-1}$  and a

secondary reflection at  $2q_4$ , thus suggesting a lamellar order with an interlayer distance of approximately 3.1 nm.

Next, the guanosine component is investigated. A distinct X-ray reflection at  $q_3 = 2.0 \text{ \AA}^{-1}$  (0.34 nm) is observed, which is characteristic of  $\pi$  stacking (Figure 1c). This finding indicates that dGMPs form  $\pi$  stacks, as there are no other chemical moieties within the composition that could interact in this way. The two dominant types of hydrogen-bonded supramolecular structures known for guanosines in supramolecular chemistry, that is, G-quartets<sup>[21a-c]</sup> and G-ribbons,<sup>[21c,d]</sup> are considered here. G-quartets typically arrange into metal-ion-stabilized hexagonal patterns of quadruplex columns,<sup>[16,21a]</sup> but related X-ray patterns were not observed here. Metal cations are usually required to stabilize guanine assemblies to form G-quartets, and, although potassium chloride was used in the preparation of the present complexes (see experimental details in the Supporting Information), it was not detected in the final complex by atomic absorption analysis, that is, K<sup>+</sup> ions were expelled from the final structure. It is therefore logical to expect some form of hydrogen-bonded G-ribbons in the present case. Note that the direct detection of the individual hydrogen bonds within the G-ribbons is not feasible in the present complicated system, which exhibits a multitude of different hydrogen bonds along the polypeptidic components and G-ribbons. Next, retrostructural modeling is used to understand how dGMPs are packed within the available “slots”, as deduced from the scattering and spectroscopic data. Note that the experimental observations provide rather stringent restrictions on the possible dGMP packing.

Figure 2c shows the suggested self-assembly, thus explaining the tetragonal antiparallel assembly of PBLG  $\alpha$  helices,  $\pi$  stacking of dGMPs, PLL  $\beta$ -sheet periodicity at 3.1 nm, and proper dimensions in all X-ray scattering measurements, which requires double folding of PLL. Figure 2d–f shows the structures in more detail. This arrangement allows, in a natural way, for the relatively narrow  $\pi$ -stacking X-ray reflection (Figure 1c), as the length of double-folded PLL (10 nm) sterically allows up to approximately 30  $\pi$ -stacking interactions in the direction parallel to the  $\beta$  sheets (Figure 2b–d). As shown in Figure 2c, d, and f, for a doubly folded PLL chain that forms a  $\beta$  sheet, each of the three neighboring lysine residues (along the direction perpendicular to the long axis of the  $\beta$  sheet) are ionically complexed with dGMP molecules. Hydrogen bonding between guanosine moieties from two neighboring  $\beta$  sheets (i.e., from “above” and “below”) leads to the formation of short G-ribbons that consist of three guanosines to match the widths of the  $\beta$  sheets, and thus corresponds to lengths based on the scattering data. Ribbon formation is further facilitated by the fact that the deoxyribose and the guanosine moieties are not coplanar and thus allows for positional adjustments.

A space-filling model generated by using molecular modeling software packages (see the Supporting Information) was utilized to optimize the geometry of G-ribbons that consist of 3 guanosines and with the above steric boundary conditions to confine them (Figure 2f). This geometry leads to hydrogen-bonding donor–acceptor distances of 0.28 nm (NH<sub>2</sub>...N)<sup>[21d]</sup> and approximately 0.33 nm (CH...O, see Fig-

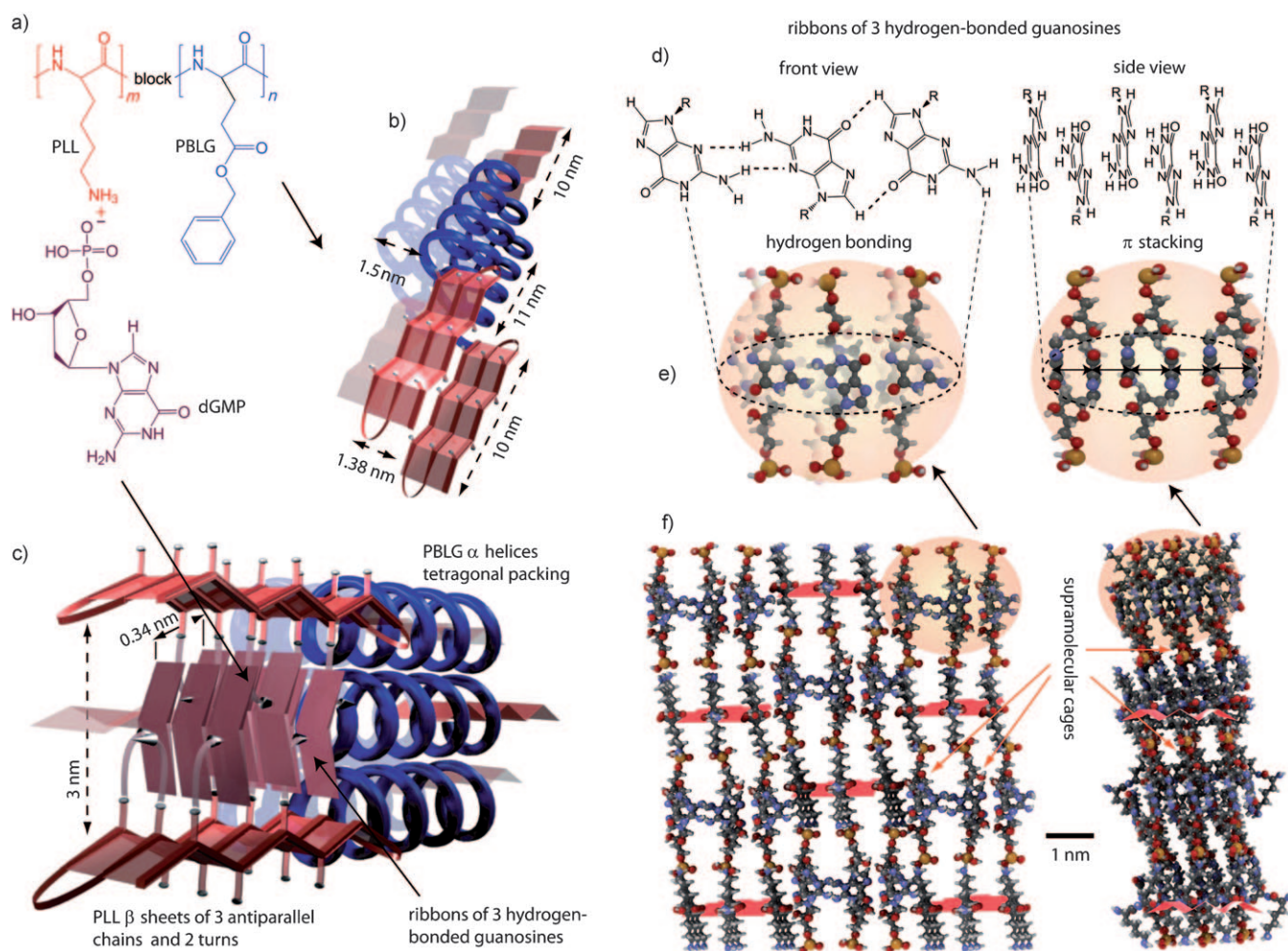


**Figure 2.** Self-assembly of diblock copolypeptide PBLG-*b*-PLL with dGMP. a) The PLL side chains are ionically complexed with dGMP. b) Antiparallel packing of the diblock copolypeptide; blue:  $\alpha$ -helical PBLG, red: PLL  $\beta$  sheet; PLL has two turns to form three antiparallel hydrogen-bonded chains. c) Guanines from three dGMPs (highlighted in brown) form hydrogen-bonded ribbons perpendicular to the  $\beta$  sheets. d, e) Suggested hydrogen bonds to form the ribbons, based on molecular models. The guanines of the dGMPs form  $\pi$  stacks along the  $\beta$  sheets. f) Illustration of the cage-like framework within the PLL(dGMP) lamellae.

ure 2c–e).<sup>[22a]</sup> Note that  $\text{CH}\cdots\text{O}$  can be considered as a weak hydrogen bond, as detected in left-handed Z-DNA, between the deoxyriboses of two closely spaced backbones of four-stranded DNA, protein–protein interfaces, and in supramolecular chemistry.<sup>[22]</sup> Note also that the suggested G-ribbon is not among the classic Type A or Type B ribbons,<sup>[21c]</sup> and is stabilized by the confinement. The height of such a dGMP ribbon together with two lysine moieties, stretched from the two opposite PLL  $\beta$  sheets is approximately 3 nm, which corresponds very well to the lamellar periodicity of 3.1 nm observed by SAXS (Figure 1d, curve 1).

However, the above structure involves steric frustration by utilizing the tetragonal assembly of PBLG helices, which acts as a template for the lateral positions of the shape-persistent PLL  $\beta$  sheets. These  $\beta$  sheets, in turn, are held in position by orthogonal shape-persistent hydrogen-bonded G-ribbons and their extended  $\pi$  stacking, hence leading to the formation of supramolecular cages. Figure 3 shows a selected segmental cut from the PLL(dGMP) domain with a total volume of approximately  $24.38 \text{ nm}^3$ , obtained by using the

molecular graphics software UCSF Chimera (see the Supporting Information). The sum of the volumes of all organic constituents within the segment (lysine strands and G-ribbons) is  $11.66 \text{ nm}^3$ . Therefore, the remaining  $12.72 \text{ nm}^3$  is assigned to free volume in the shown segment and thus, the porosity within the PLL(dGMP) is suggested to be approximately 52%. The framework contains different cages, the heights and widths of which vary as follows: 1.5 nm and 1 nm, and 1.2 nm and approximately 0.8 nm (see Figure 2f, left); 1 nm and 0.6 nm, and 1.2 nm and 0.4 nm (see Figure 2f, right). The different cages are lined differently by polar moieties, such as amines from guanines and ethers and hydroxy groups from the sugar rings.

Direct evidence of the pores is obtained by monitoring the concentration of the non-absorbed fraction of a dissolved model dye in an immersed PBLG-*b*-PLL(dGMP) sample by using UV/Vis spectroscopy. Initially, 6 mol % of 4-nitroaniline (4NA, see Figure S2) per lysine residues of PLL was dissolved in water, and after 5, 10, and 15 days, 66 %, 76 %, and 90 % of 4NA, respectively, was absorbed by the porous PBLG-*b*-



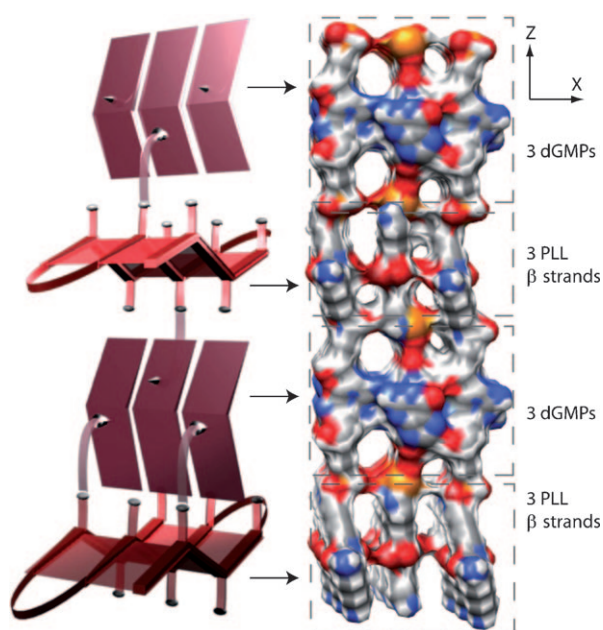


**Figure 3.** Suggested supramolecular cage-like pores within the PLL-(dGMP) domains, shown in a segmental front-view cut, as computed and visualized by UCSF Chimera molecular modeling package (right). Simplified schematic front view of the self-assembly within the segment (left).

PLL(dGMP) (see Figure S3a). In contrast, essentially no absorption was observed for pure PBLG-*b*-PLL because of the absence of the pores. Selectivity could be demonstrated by using an equimolar aqueous mixture of two dyes, that is, 4NA and ethyl orange (EO, see Figure S2). During the first 5 days both dyes were absorbed similarly in terms of quality (see Figure S3b), but after 15 days, essentially all 4NA had been replaced by EO within the cages. The cages are therefore selective for EO over 4NA, probably caused by stronger interactions with the cage interior because of its sulfonate and hydrogen-bonding accepting groups.

To summarize: 1) The first route to polymeric supramolecular framework materials has been shown, which leads to supramolecular cages based on organic polymers. 2) The polymeric units show robustness (compared to oligomeric supramolecular framework solids). Combination of directed noncovalent interactions (hydrogen bonding and  $\pi$  stacking), less directional interactions (electrostatic interactions and hydrophobic packing), and relatively rigid ordered templating scaffolds ( $\alpha$  helix and  $\beta$  sheet) leads to packing frustration. The framework assembles quickly as a precipitate after mixing the starting components and solvent removal and does not require a slow crystallization process. 3) The material shows multilevel hierarchical self-assembly and is the first example of guanosine ribbons incorporated in polymeric self-assembly. 4) Models suggest that the framework consists of interconnected cages with different functionalities at the cage wall, thus extending in two perpendicular directions. The various functionalities of the cage walls arise from the G-ribbon motif within the multicompartment 3D space, as the typical cage sizes are expected to be approximately 1.5 nm. 5) The polymeric supramolecular

framework allows incorporation and release of small molecular objects in a selective manner.

The work presented herein is expected to inspire other types of polymeric supramolecular framework materials based on orthogonal shape-persistent supramolecular motifs, denoted as “woodpile assembly”. The combined effects of the directed hydrogen bonds, shape persistence, and packing frustrations are relevant design motifs that lead to a generic route for tunable nanoscale cages. It is expected that the cage sizes can be tuned by modifying the block copolymer molecular lengths and the architectures, and by using different nucleotides and their complements. Most interestingly, routes could be envisioned where cages with different “philicities” can be prepared simultaneously, which could open new possibilities for, for example, selective absorption and chemical synthesis within the cages.

Received: November 16, 2010

Published online: February 14, 2011

**Keywords:** nanomaterials · nucleotides · porous materials · self-assembly · supramolecular chemistry

- [1] a) S. R. Batten, R. Robson, *Angew. Chem.* **1998**, *110*, 1558; *Angew. Chem. Int. Ed.* **1998**, *37*, 1460; b) J. Seo, D. Whang, H. Lee, S. Jun, J. Oh, Y. Jeon, K. Kim, *Nature* **2000**, *404*, 982; c) S. R. Batten, K. S. Murray, *Coord. Chem. Rev.* **2003**, *246*, 103; d) A. Proust, R. Thouvenot, P. Gouzerh, *Chem. Commun.* **2008**, 1837; e) M. B. Duriska, S. M. Neville, J. Lu, S. S. Iremonger, J. F. Boas, C. J. Kepert, S. R. Batten, *Angew. Chem.* **2009**, *121*, 9081; *Angew. Chem. Int. Ed.* **2009**, *48*, 8919.
- [2] M. Yoshizawa, J. K. Klosterman, M. Fujita, *Angew. Chem.* **2009**, *121*, 3470; *Angew. Chem. Int. Ed.* **2009**, *48*, 3418.
- [3] P. Mal, B. Breiner, K. Rissanen, J. R. Nitschke, *Science* **2009**, *324*, 1697.
- [4] S. Ma, D. Sun, J. M. Simmons, C. D. Collier, D. Yuan, H. C. Zhou, *J. Am. Chem. Soc.* **2008**, *130*, 1012.
- [5] C. J. Kepert, *Chem. Commun.* **2006**, 695.
- [6] D. Carriazo, F. Pico, M. C. Gutierrez, F. Rubio, J. M. Rojo, F. del Monte, *J. Mater. Chem.* **2010**, *20*, 773.
- [7] A. Knoesen, G. Song, W. Volksen, E. Huang, T. Magbitang, L. Sundberg, J. Heidrick, C. Hawker, R. Miller, *J. Electron. Mater.* **2004**, *33*, 135.
- [8] a) S. Kitagawa, R. Kitaura, S. Noro, *Angew. Chem.* **2004**, *116*, 2388; *Angew. Chem. Int. Ed.* **2004**, *43*, 2334; b) N. Malek, Th. Maris, M.-E. Perron, J. D. Wuest, *Angew. Chem.* **2005**, *117*, 4089; *Angew. Chem. Int. Ed.* **2005**, *44*, 4021; c) C. Trolliet, G. Poulet, A. Tuel, J. D. Wuest, P. Sautet, *J. Am. Chem. Soc.* **2007**, *129*, 3621; d) P. Dechambenoit, S. Ferlay, N. Kyritsakas, M. W. Hosseini, *J. Am. Chem. Soc.* **2008**, *130*, 17106.
- [9] a) D. Bradshaw, J. B. Claridge, E. J. Cussen, T. J. Prior, M. J. Rosseinsky, *Acc. Chem. Res.* **2005**, *38*, 273–282; b) M. Kawano, M. Fujita, *Coord. Chem. Rev.* **2007**, *251*, 2592; c) Q. Li, W. Zhang, O. Miljanic, C. Sue, Y. Zhao, L. Liu, C. B. Knobler, J. Stoddart, O. Yaghi, *Science* **2009**, *325*, 855–859; d) Y. Inokuma, T. Arai, M. Fujita, *Nat. Chem.* **2010**, *2*, 780.
- [10] C. B. Aakeröy, A. M. Beatty, D. S. Leinen, *Angew. Chem.* **1999**, *111*, 1932; *Angew. Chem. Int. Ed.* **1999**, *38*, 1815.
- [11] a) A. Thomas, A. Fischer, F. Goettmann, M. Antonietti, J.-O. Mueller, R. Schlögl, J. M. Carlsson, *J. Mater. Chem.* **2008**, *18*, 4893; b) P. Kuhn, M. Antonietti, A. Thomas, *Angew. Chem.* **2008**, *120*, 3499; *Angew. Chem. Int. Ed.* **2008**, *47*, 3450; c) C. E. Chan-Thaw, A. Villa, P. Katekomol, D. Su, A. Thomas, L. Prati, *Nano*

- Lett.* **2010**, *10*, 537; d) H. Furukawa, O. Yaghi, *J. Am. Chem. Soc.* **2009**, *131*, 8875.
- [12] a) P. M. Budd, N. B. McKeown, D. Fritsch, *J. Mater. Chem.* **2005**, *15*, 1977–1986; b) M. Carta, K. J. Msayib, N. McKeown, *Tetrahedron Lett.* **2009**, *50*, 5954–5957; c) P. M. Budd, N. B. McKeown, *Polym. Chem.* **2010**, *1*, 63.
- [13] a) T. Thurn-Albrecht, J. Schotter, G. A. Kästle, N. Emley, T. Shibauchi, L. Krusin-Elbaum, K. Guarini, C. T. Black, M. T. Tuominen, T. P. Russell, *Science* **2000**, *290*, 2126; b) M. A. Hillmyer, *Adv. Polym. Sci.* **2005**, *190*, 137; c) L. Chen, W. A. Phillip, E. L. Cussler, M. A. Hillmyer, *J. Am. Chem. Soc.* **2007**, *129*, 13786; d) S. Valkama, A. Nykänen, H. Kosonen, R. Ramani, F. Tuomisto, P. Engelhardt, G. ten Brinke, O. Ikkala, J. Ruokolainen, *Adv. Funct. Mater.* **2007**, *17*, 183.
- [14] a) T. F. A. De Greef, E. W. Meijer, *Nature* **2008**, *453*, 171; b) O. Ikkala, G. ten Brinke, *Science* **2002**, *295*, 2407; c) P. Cordier, F. Tournilhac, C. Soulié-Ziakovic, L. Leibler, *Nature* **2008**, *451*, 977.
- [15] Note that in supramolecular science occasionally chainlike entities embedded in the crystal lattice are denoted as polymers. They do not form chains beyond the lattice. By contrast, in this work distinct polymers are used as tectons.
- [16] N. Houbenov, A. Nykänen, H. Iatrou, N. Hadjichristidis, J. Ruokolainen, C. F. J. Faul, O. Ikkala, *Adv. Funct. Mater.* **2008**, *18*, 2041.
- [17] Circular dichroism (CD) spectroscopy unfortunately cannot be applied for bulky solid samples, and hence it is not reliable for the present case.
- [18] a) H. Schlaad, *Adv. Polym. Sci.* **2006**, *202*, 53; b) Also PBLG is able to form  $\beta$  sheets, but only for short chain lengths of less than 20 units. Otherwise, the stabilization of the PBLG chains in the  $\alpha$ -helical secondary conformation is typically observed.
- [19] The calculated layer thickness is based on ideal PBLG helical structure, that is, a helix without kinks. Kinks can emerge along the helical rod, though, therefore PBLG can be slightly extended, and hence, PLL(dGMP) slightly reduced, thus keeping the total periodicity.
- [20] A. Douy, B. Gallot, *Polymer* **1982**, *23*, 1039.
- [21] a) J. T. Davis, *Angew. Chem.* **2004**, *116*, 684; *Angew. Chem. Int. Ed.* **2004**, *43*, 668; b) B. H. Ozer, B. Smarsly, M. Antonietti, C. F. J. Faul, *Soft Matter* **2006**, *2*, 329; c) S. Pieraccini, S. Masiero, O. Pandoli, P. Samori, G. P. Spada, *Org. Lett.* **2006**, *8*, 3125; d) A. Calzolaria, R. Di Felicea, E. Molinaria, A. Garbesi, *Phys. E* **2002**, *13*, 1236.
- [22] a) L. Jiang, L. Lai, *J. Biol. Chem.* **2002**, *277*, 37732; b) M. Egli, R. V. Gessner, *Proc. Natl. Acad. Sci. USA* **1995**, *92*, 180.